Asia-Pac. J. Atmos. Sci., 52(2), 191-208, 2016
DOI:10.1007/s13143-016-0019-7
pISSN 1976-7633 / eISSN 1976-7951

Projected Rainfall and Temperature Changes over Malaysia at the end of the 21st Century based on PRECIS Modelling System

Jui Le Loh[1,3], Fredolin Tangang[1], Liew Juneng[1], David Hein[2], and Dong-In Lee[3]

[1]*School of Environmental and Natural Resource Sciences, Faculty of Science and Technology, Universiti Kebangsaan Malaysia, Selangor, Malaysia*
[2]*Met Office Hadley Centre for Climate Science and Services, Exeter, Devon, UK*
[3]*Division of Earth Environmental System Science (Major of Environmental Atmosphere Sciences), Pukyong National University, Busan, Korea*

(Manuscript received 15 October 2015; accepted 15 April 2016)

Abstract: This study investigates projected changes in rainfall and temperature over Malaysia by the end of the 21st century based on the Intergovernmental Panel on Climate Change (IPCC) Special Report on Emission Scenarios (SRES) A2, A1B and B2 emission scenarios using the Providing Regional Climates for Impacts Studies (PRECIS). The PRECIS regional climate model (HadRM3P) is configured in $0.22^{o} \times 0.22^{o}$ horizontal grid resolution and is forced at the lateral boundaries by the UKMO-HadAM3P and UKMO-HadCM3Q0 global models. The model performance in simulating the present-day climate was assessed by comparing the model-simulated results to the Asian Precipitation - Highly-Resolved Observational Data Integration Towards Evaluation (APHRODITE) dataset. Generally, the HadAM3P/PRECIS and HadCM3Q0/PRECIS simulated the spatio-temporal variability structure of both temperature and rainfall reasonably well, albeit with the presence of cold biases. The cold biases appear to be associated with the systematic error in the HadRM3P. The future projection of temperature indicates widespread warming over the entire country by the end of the 21st century. The projected temperature increment ranges from 2.5 to 3.9°C, 2.7 to 4.2°C and 1.7 to 3.1°C for A2, A1B and B2 scenarios, respectively. However, the projection of rainfall at the end of the 21st century indicates substantial spatio-temporal variation with a tendency for drier condition in boreal winter and spring seasons while wetter condition in summer and fall seasons. During the months of December to May, ~20-40% decrease of rainfall is projected over Peninsular Malaysia and Borneo, particularly for the A2 and B2 emission scenarios. During the summer months, rainfall is projected to increase by ~20-40% across most regions in Malaysia, especially for A2 and A1B scenarios. The spatio-temporal variations in the projected rainfall can be related to the changes in the weakening monsoon circulations, which in turn alter the patterns of regional moisture convergences in the region.

Key words: Climate change, dynamical downscaling, Malaysian climate, regional climate projections, PRECIS, HadRM3P

1. Introduction

The Intergovernmental Panel on Climate Change (IPCC) concluded in its Fifth Assessment Report (AR5) that climate change is unequivocal and is primarily due to the cumulative concentration of anthropogenic greenhouse gasses in atmosphere (IPCC, 2013). For adaptation to climate change, information at regional and local scales is crucially important. Generally, the IPCC AR5 and other previous IPCC reports provided climate changes assessments at the global scale, but knowledge gaps remain large at both regional and local scales. Malaysia, in particular, is still lacking in detailed climate change information (Tangang et al., 2012). Hence, this research aims for enhancing the regional and local knowledge of future climate change.

Malaysia is located in the western Maritime Continent where its climate and weather are modulated largely by the Asian-Australian monsoon system (Aldrian and Susanto, 2003; Chang et al., 2003; McBride et al., 2003; Moron et al., 2009; Robertson et al., 2011; Juneng and Tangang, 2010; Tangang et al., 2012). However, in addition to the cyclic monsoon cycle, the climate over this region also experiences substantial intra-seasonal to interannual variabilities associated with Madden-Julian oscillation (MJO), Indian Ocean Dipole (IOD) and El-Niño Southern Oscillation (ENSO) (Ashok et al., 2001; Hendon, 2003; McBride et al., 2003; Waliser et al., 2003; Wang et al., 2003; Tangang and Juneng, 2004; Chang et al., 2005; Juneng and Tangang, 2005; Tangang et al., 2007; Behera et al., 2008; Meehl and Arblaster, 2011; Tangang et al., 2012; Salimun et al., 2014, 2015). Moreover, previous studies also indicated possible long-term changes of the monsoon system, which could be associated with warming of global climate in recent decades (Hu et al., 2000a, 2000b; Gong and Ho, 2002; Meehl and Arblaster, 2003; Xu et al., 2006; Meehl et al., 2007; Trenberth et al., 2007; Wu et al., 2007; Yu and Zhou, 2007; Juneng and Tangang, 2010).

Future climate according to greenhouse gas emission scenarios can be projected using coupled atmosphere-ocean general circulation models (AOGCMs) (Ravindranath and Sathaye, 2002; IPCC, 2007, 2013). Despite considerable inter-model differences, the AOGCMs have shown encouraging steady improvement over the last decades (Rupa Kumar et al., 2006; Randall et al., 2007; Giorgi et al., 2009). The projected future climate scenarios reported in the AR5 were based on over forty AOGCMs under the auspices of the Coupled Model

Corresponding Author: Fredolin Tangang, School of Environmental and Natural Resource Sciences, Faculty of Science and Technology, Universiti Kebangsaan Malaysia, 43600 Bangi, Selangor, Malaysia.
E-mail: tangang@ukm.edu.my

Intercomparison Project 5 (CMIP5) (IPCC, 2013). However, despite their ability to simulate climate at the global and continental scales, the capability of these models is quite limited in resolving the local-level details generally required for impact assessment (e.g. Takle et al., 1999; Jones et al., 2004; Randall et al., 2007). At such coarse resolution, important processes that are influenced by topography and landmass distribution are often not well simulated. Regional climate models (RCMs) may be used to dynamically downscale AOGCMs to produce more detailed climatic information for a particular region (e.g. Giorgi and Hewitson, 2001; Jones et al., 2004). With horizontal resolutions of typically 10-50 km, a regional model covers limited areas of the globe, with input lateral boundary conditions provided by AOGCMs (Dickinson et al., 1989). Currently, studies on regional climate downscaling over Malaysia are limited (Tangang et al., 2012). A recent study by Kwan et al. (2014) reported that the Providing Regional Climate for Impacts Studies (PRECIS) modelling system provides a reasonable simulation of regional and local climate over Malaysia for a period of 1970-1999.

The present study examines the projected changes of seasonal precipitation and temperature by the end of the 21st century over Malaysia regions based on IPCC SRES A2, A1B and B2 emission scenarios. The PRECIS regional climate model (HadRM3P), nested within the UKMO HadAM3P and HadCM3Q0 global models, is used to simulate regional rainfall and temperature for future climate projections. The next section describes briefly the model, data and analysis employed in the study. Section 3 elaborates and discusses the simulation results, model validation and future climate projections. Finally, Section 4 summarizes and concludes the study.

2. Data and method

The study employs PRECIS, a regional climate modelling system developed by the Hadley Centre of the United Kingdom Met Office (UKMO) (Jones et al., 2004). The main component of PRECIS is HadRM3P (Jones et al., 2004; Massey et al., 2015), a high resolution atmosphere-land surface coupled model (Jones et al., 2004) that has 19 hybrid vertical coordinate levels and uses a hydrostatic dynamic. Detailed description of the model is provided by Jones at al. (2004) and Massey et al. (2015). In a recent study, Kwan et al. (2014) used the same model and domain configuration to downscale the second generation of the European Centre for Medium Range Weather Forecast (ECMWF) reanalysis (ERA40). In the current study, HadRM3P is forced at the lateral boundaries by the Hadley Centre Atmospheric General Circulation Model 3P (HadAM3P) and Hadley Centre perturbed physics ensemble (HadCM3Q0, "0" means the standard or unperturbed model) with N96 resolution (1.25 × 1.875 degrees).

The HadCM3Q0 and HadAM3P models are developed by the Hadley Centre UKMO (Gordon et al., 2000; Pope et al., 2000; Collins et al., 2001; Massey et al., 2015). HadCM3Q0 was developed from the earlier Hadley Centre Coupled Model

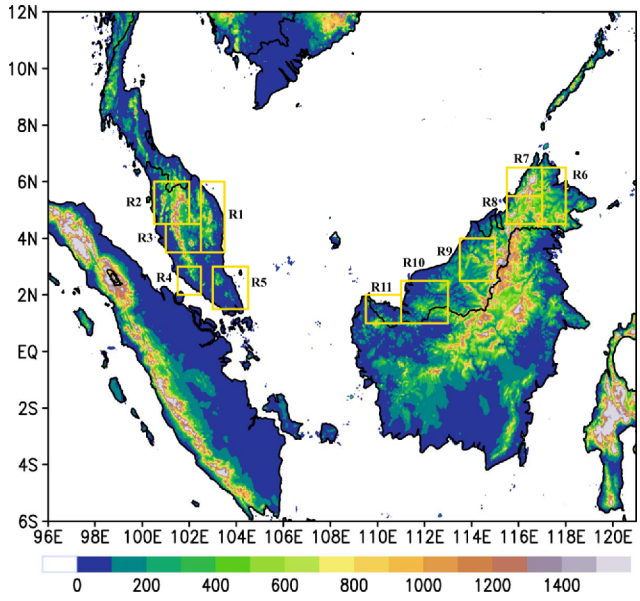

Fig. 1. The geographical extent of the domain used for HadAM3P/PRECIS and HadCM3Q0/PRECIS simulations. The boxes represent the 11 sub-regions selected for area-averaged analysis. The elevation is in meter.

version 3 (HadCM3) model (Johns et al., 1997; Massey et al., 2015), but with various improvements to the atmosphere and ocean components such as increasing the horizontal resolution of the HadCM3 model. HadCM3Q0 is a coupled GCM which has been derived from the atmospheric component of HadCM3. The oceanic component of the model has 20 levels with a horizontal resolution of 1.25° × 1.25° (Johns et al., 2003). The HadAM3P is a global atmosphere-only model, which was developed based on the previous version of the HadAM2b climate model (Stratton, 1999), with some major improvements (Pope et al., 2000). In the current study the HadRM3P is configured for a domain extending from 96°E to 121°E and 6°S to 12°N (Fig. 1) with a total horizontal grids of 135 × 100, covering both Peninsular Malaysia and Borneo. HadRM3P was run at 0.22° × 0.22° (~25 km resolution) horizontal resolution with lateral boundary conditions provided from the HadAM3P and HadCM3Q0 simulations. The baseline climate simulation covers a period of 25 years from 1966-1990. For future simulation, time slices from a 30 years period (2070-2099) are considered. Future simulations using IPCC SRES A2 and B2 scenarios utilise HadAM3P, while SRES A1B emissions utilise HadCM3Q0. The A2 and B2 represent the emission scenarios of regionally focused development but with priority to economic and environmental issues, respectively, while A1B represents emission scenario of globally focused technological change (Nakićenović et al., 2000). For the HadAM3P driven PRECIS simulation (hereafter HadAM3P/PRECIS), the sea-surface boundary conditions are derived by combining changes in the sea-surface temperature simulated in the integrations of UKMO's HadCM3Q0 using the same emissions scenarios with the historically observed Hadley

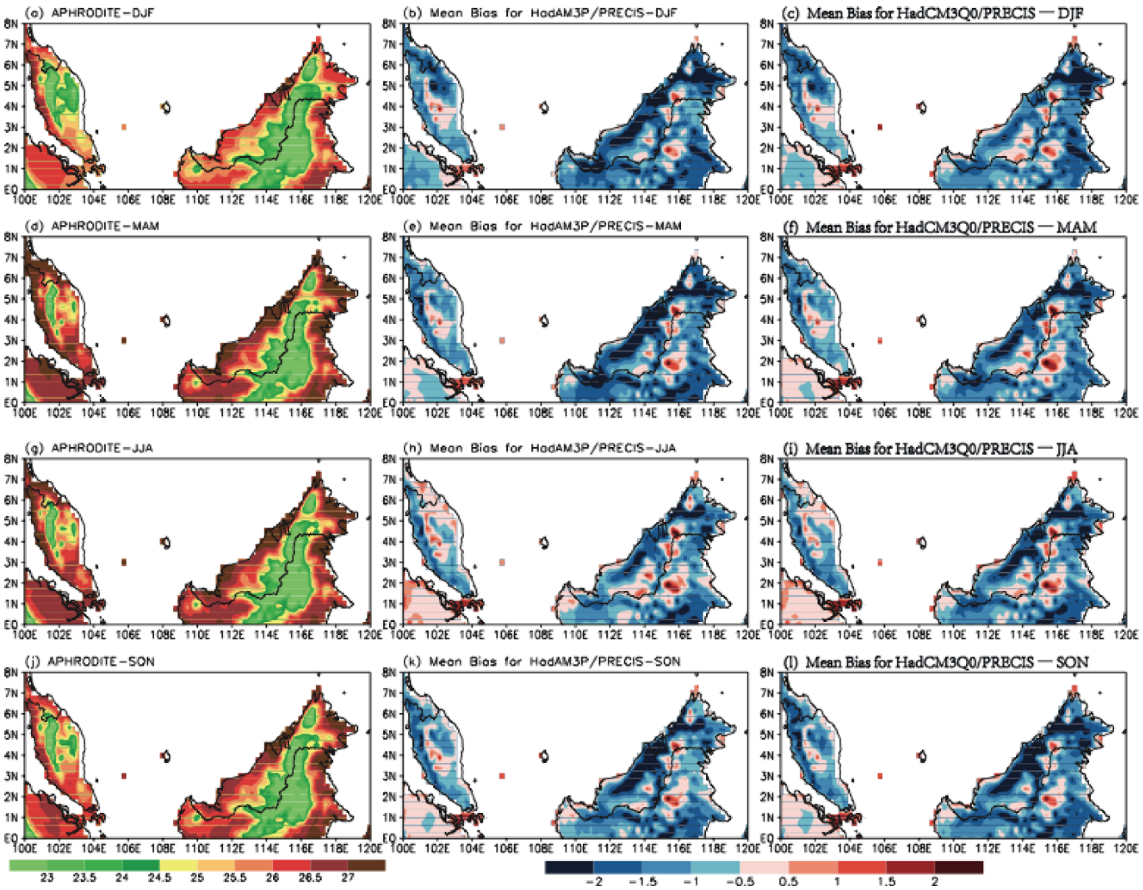

Fig. 2. Spatial distributions of APHRODITE seasonal mean temperature (°C) (left panel), HadAM3P/PRECIS biases (middle panel) and HadCM3Q0/PRECIS biases (right panel) for the baseline period simulation.

Centre Global Ice and Sea Surface Temperature (HadISST) time series. For the HadCM3Q0 driven PRECIS simulation based on the A1B scenarios (hereafter HadCM3Q0/PRECIS), the sea-surface boundary conditions are taken directly from the ocean component of the HadCM3Q0 run.

The HadAM3P/PRECIS and HadCM3Q0/PRECIS simulations during the baseline period were validated with the $0.25^{o} \times 0.25^{o}$ the Asian Precipitation - Highly-Resolved Observational Data Integration Towards Evaluation (APHRODITE) gridded data (Yatagai et al., 2012). APHRODITE dataset has been validated against observation over Malaysia and was found to be one of the best performed products (Tan et al., 2015). For detailed characterization of future climate changes in Malaysia, eleven sub-regions were selected to represent specific regions of interest in both the Peninsular Malaysia and northern Borneo (Fig. 1). These sub-regions are identical to those considered in Kwan et al. (2014).

3. Results and discussion

a. Validation of baseline climate simulations

(1) Mean Surface Mean Air Temperature

Malaysia experiences minimum and maximum mean surface air temperature during December and May, respectively (Tangang et al., 2007). During December, mean surface air temperature averages 25-26°C, with cooler temperature over the east coast of Peninsular Malaysia due to the advection of cool air masses by the northeasterlies during winter monsoon. During May, the mean temperature ranges from 26°C to 28°C. Figure 2 depicts the spatial comparison between the APHRODITE gridded seasonal mean temperature and the mean biases of HadAM3P/PRECIS and HadCM3Q0/PRECIS over Malaysia from 1966 to 1990. Generally, HadAM3P/PRECIS and HadCM3Q0/PRECIS simulate reasonably well the spatial distribution of the seasonal mean temperatures but with cold biases in most areas, consistent with the ERA40/PRECIS simulation described in Kwan et al. (2014; Fig. 2). Given the fact that these two studies share the same model and domain configuration but with different forcings, the sources of biases may be common for both studies. To further investigate the likely reasons for these cold biases, we plotted in Fig. 3 the HadCM3Q0 biases against the APHRODITE temperature data. The figure indicates overall warm biases of HadCM3Q0 compared to cold biases of PRECIS simulation (Fig. 2). Such opposite polarity of biases between GCM and RCM suggests some processes in the RCM may cause such responses. Figure 4 depicts the differences of shortwave

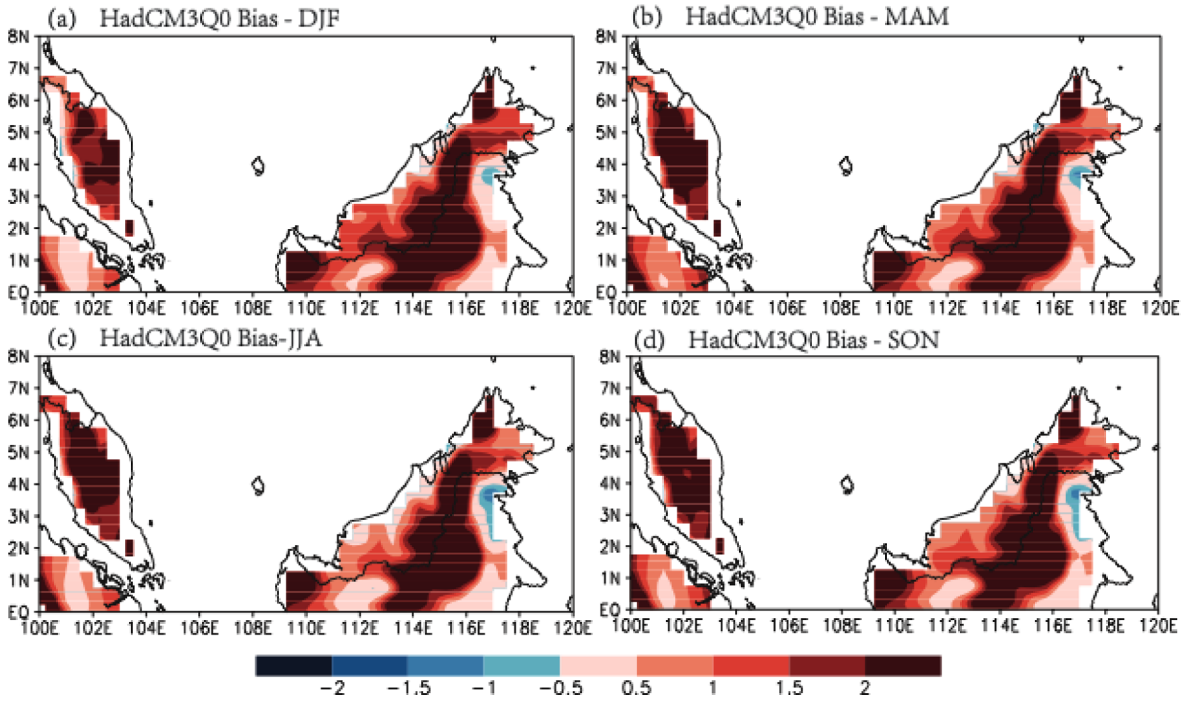

Fig. 3. The spatial distribution of HadCM3Q0 temperature biases (°C) with reference to APHRODITE at different seasons.

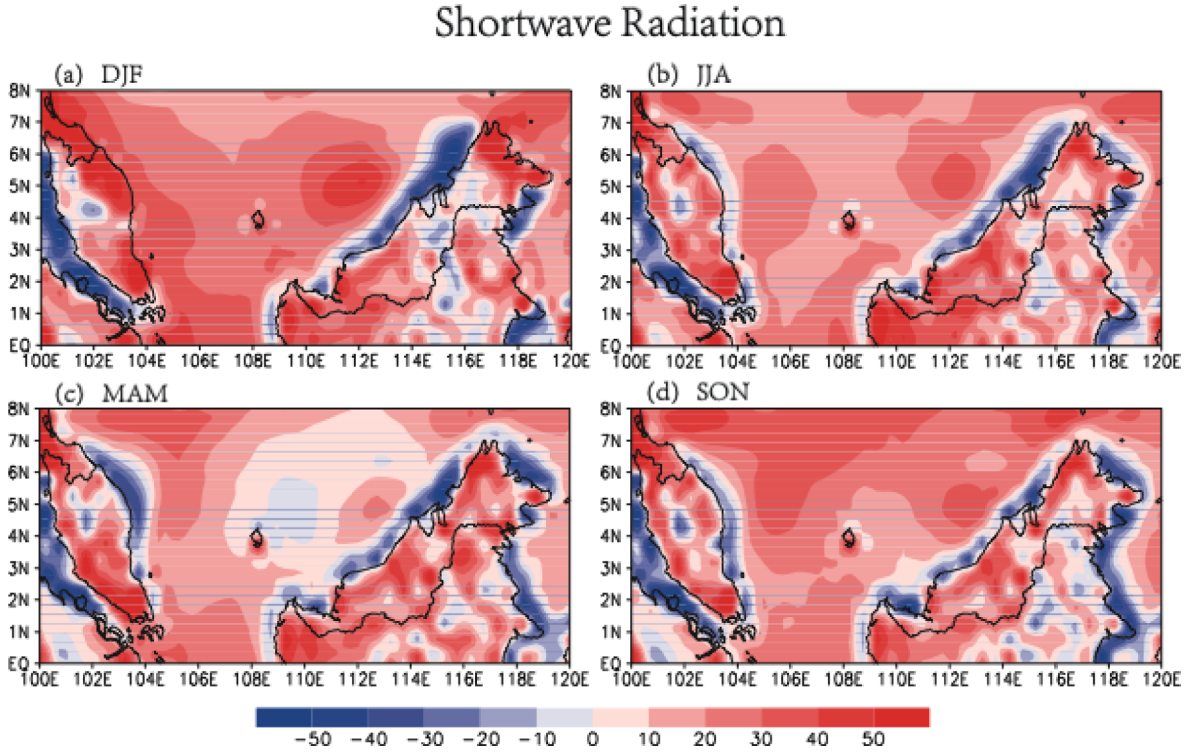

Fig. 4. The distribution of shortwave radiation difference between the HadCM3Q0 and the HadCM3Q0/PRECIS (HadCM3Q0 minus HadCM3Q0/PRECIS) at different seasons. Unit is W m^{-2}.

radiation between HadCM3Q0 and HadCM3Q0/PRECIS. It is noted that the driving HadCM3Q0 is warmed by much larger shortwave fluxes compared to PRECIS over both Peninsular Malaysia and Borneo except over the central Peninsular Malaysia and central Borneo where the HadCM3Q0/PRECIS simulation produces warm biases. Hence, the cold biases in

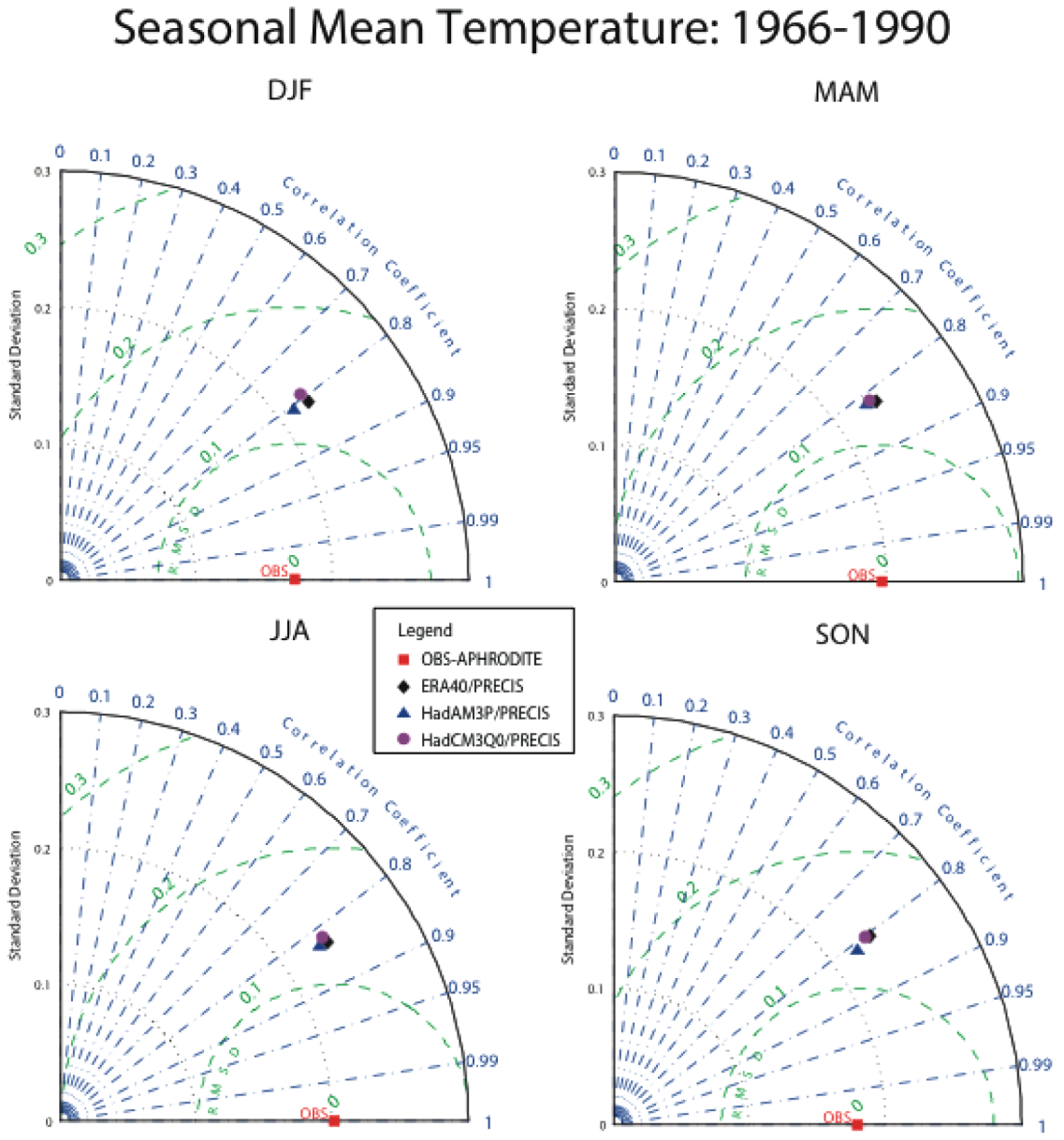

Fig. 5. The distribution of shortwave radiation difference between the HadCM3Q0 and the HadCM3Q0/PRECIS (HadCM3Q0 minus HadCM3Q0/PRECIS) at different seasons. Unit is W m^{-2}.

PRECIS are partially accounted by shortcomings in the surface shortwave radiation processes. Hudson and Jones (2002) highlighted cold biases may result from negative feedbacks between increased cloudiness and reduction in shortwave radiation and insolation reaching the earth's surface.

Figure 5 shows the Taylor diagrams comparing the seasonal spatial correlation, root-mean-square-error and standard deviations of mean surface air temperature of HadAM3P/PRECIS, HadCM3Q0/PRECIS and ERA40/PRECIS versus the APHRODITE dataset for the baseline period. The ERA40/PRECIS simulation was obtained from Kwan et al. (2014). Overall, the performances of HadAM3P/PRECIS and HadCM3Q0/PRECIS are consistent with those of ERA40/PRECIS. For all seasons, the spatial correlation values are relatively high (~0.80). This result shows that both models, HadAM3P/PRECIS and HadCM3Q0/PRECIS, perform reasonably well in simulating the seasonal mean temperature over Malaysia during the baseline period.

The seasonal cycles of observed APHRODITE and simulated HadAM3P/PRECIS and HadCM3Q0/PRECIS temperatures of the 11 sub-regions are compared in Fig. 6. Consistent with Fig. 2, both HadAM3P/PRECIS and HadCM3Q0/PRECIS tend to underestimate the mean temperature over these sub-regions, particularly including R2 of northern Peninsular Malaysia and R6, R8, R9 and R10 of Borneo. However, in sub-regions R1, R3, R4, R5, R7, both models

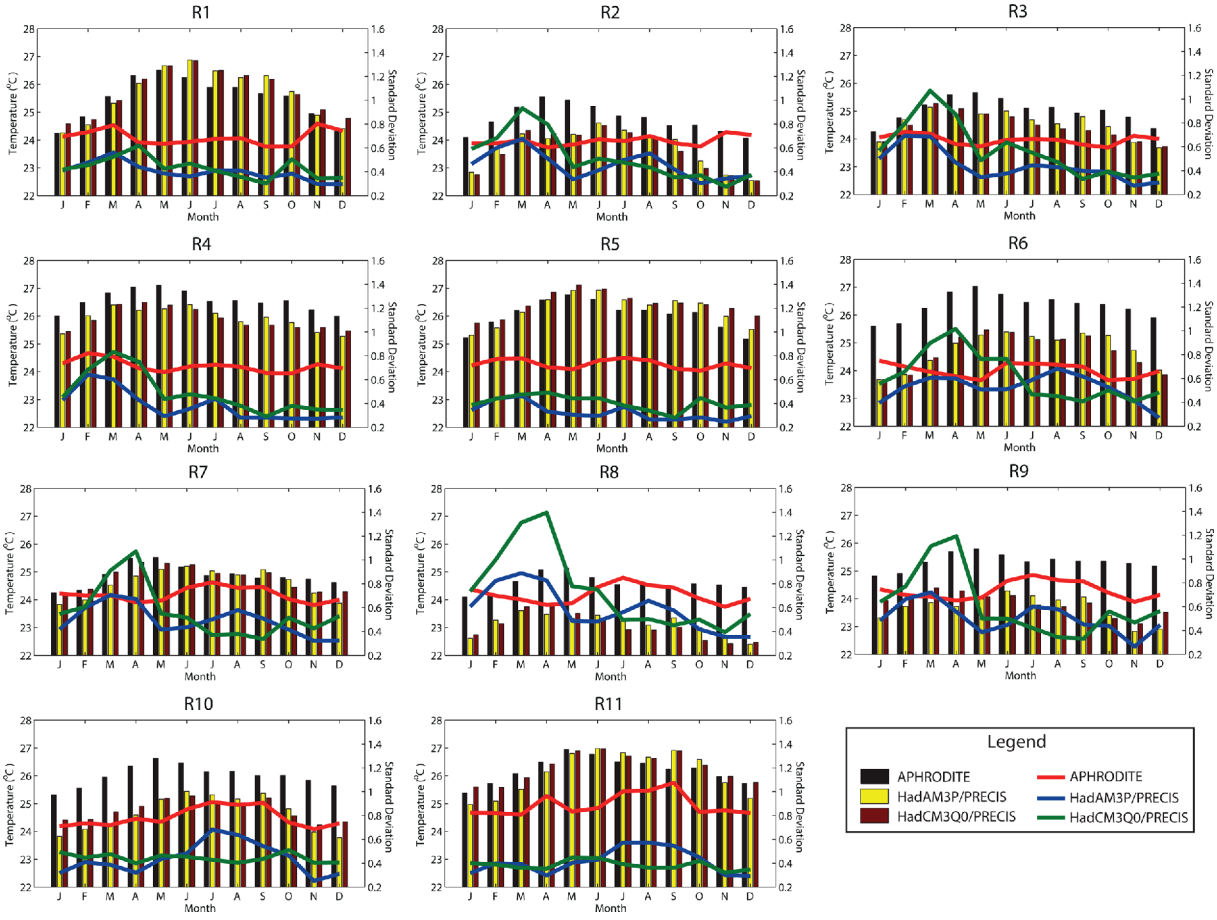

Fig. 6. Comparison between averaged baseline monthly temperature climatology (left ordinate) of the APHRODITE data and the HadAM3P/PRECIS and HadCM3Q0/PRECIS downscaling simulation, over the 11 sub-regions (refer Fig. 1). The observed and simulated interannual variabilities as indicated by the year-to-year standard deviations (right ordinate) are also plotted.

performed reasonably well. There is also a mismatch of the timings of maximum and minimum warming between models and APHRODITE data in some sub-regions. For example, in R1 sub-region, the simulated maximum temperature of both models occurs in July compared to May in the observed cycle. Similarly, in some sub-regions the simulated minimum temperature occurs in February instead of December or January in the observation. However, in R3 sub-region, the opposite occurs where the simulated temperature peaks in March compared to May in APHRODITE. The standard deviations reflecting the interannual variability of the mean temperature of the sub-regions are also shown in Fig. 6. HadAM3P/PRECIS and HadCM3Q0/PRECIS generally underestimated the APHRODITE standard deviations. However in most regions, the HadAM3P/PRECIS and HadCM3Q0/PRECIS show maximum interannual variability during the MAM period instead of during the DJF as reported in Tangang et al. (2007). The interannual variability of HadAM3P/PRECIS and HadCM3Q0/PRECIS simulations may be dependent on the characteristics of interannual variability of the forcing GCMs. Since the main interest of this study is on the mean change associated with different SRES emission scenarios, detailed understanding of interannual variability in the forcing GCMs is beyond the scope of this study.

(2) Monthly rainfall

The downscaled HadAM3P/PRECIS and HadCM3Q0/PRECIS precipitation outputs are compared with APHRODITE gridded data in Fig. 7. Generally, the simulated seasonal rainfall of both models show spatio-temporal variations. The HadAM3P/PRECIS tends to underestimate seasonal rainfall in western Borneo and Peninsular Malaysia during DJF and in western Borneo during SON. During MAM and JJA, the HadAM3P/PRECIS performed reasonably well over Borneo but underestimated rainfall over east coast Peninsular Malaysia. In contrast, the HadCM3Q0/PRECIS overestimated the seasonal rainfall, particularly over the central Borneo. However, it also showed dry condition over northern and eastern Borneo during DJF. During SON, the variation is consistent with that of the HadAM3P/PRECIS except the simulated condition is less dry. In both models, there is a tendency for overestimation of rainfall over some mountainous areas. Kwan et al. (2014) noted a similar overestimation of the precipitation over the mountainous area. As highlighted in

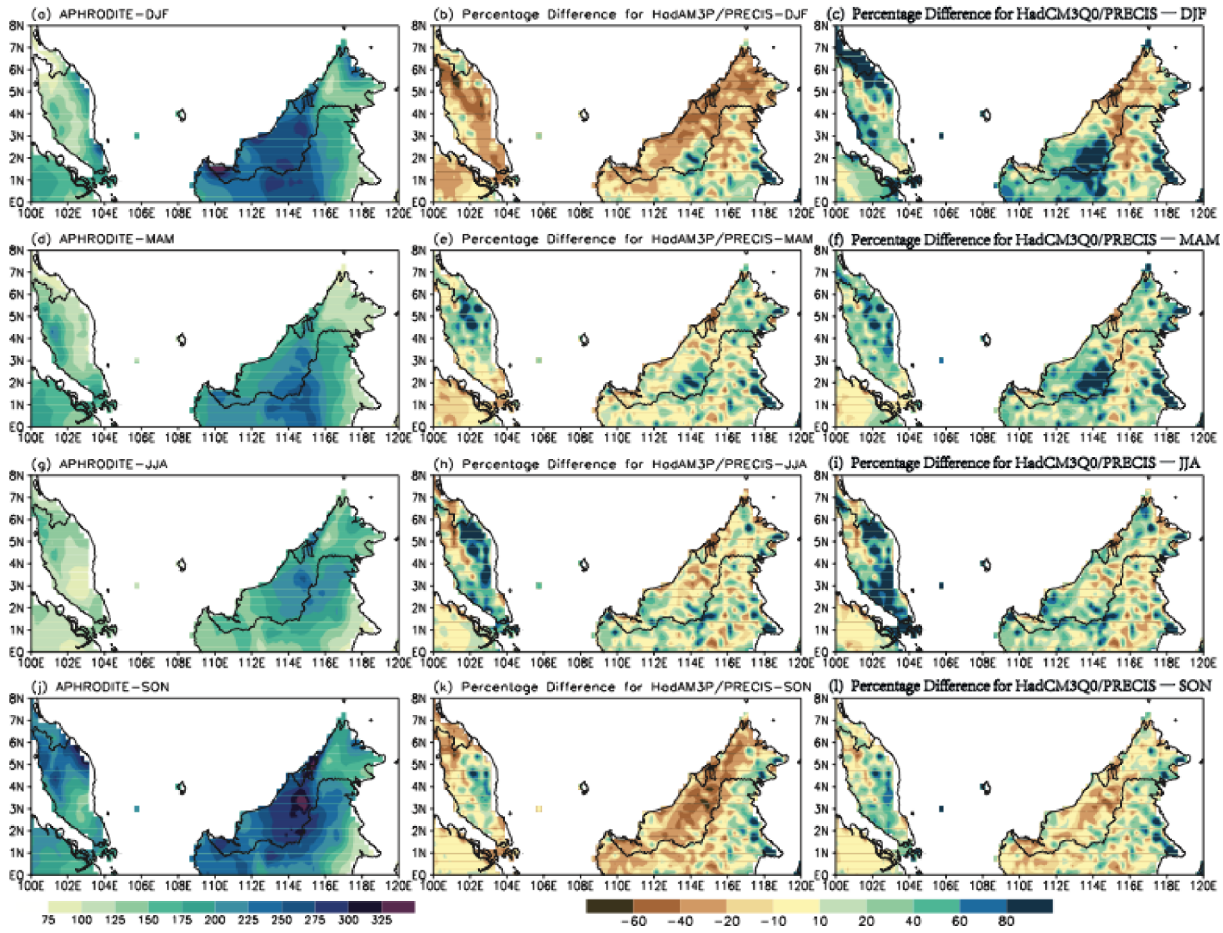

Fig. 7. Spatial distributions of APHRODITE seasonal mean rainfall (mm) (left panel), HadAM3P/PRECIS biases (middle panel) and HadCM3Q0/PRECIS biases (right panel) for the baseline period simulation. The biases are indicated in unit of percentages of seasonal APHRODITE means.

other studies, this could be due to model's low resolution, misrepresentation of land - surface processes and their interactions in the model (e.g. Alves and Marengo, 2010).

The underestimation of rainfall in the HadAM3P/PRECIS during SON and DJF, which is ~ −60% of observed rainfall, may indicate the model's failure in simulating the winter monsoon rainfall and the rain producing system discussed in Chen et al. (2013). In contrast, HadCM3Q0/PRECIS overestimated the winter monsoon rainfall in most areas especially in northeastern Peninsular Malaysia and central Borneo. The HadCM3Q0/PRECIS also tends to underestimate rainfall over eastern Borneo. These discrepancies may be related to the feedback processes in the model. The relatively dry (wet) area in eastern (central) Borneo corresponds well to area of larger (smaller) sensible heat flux (not shown). Generally, the HadAM3P/PRECIS performance tends to be better during MAM where the simulated spatial pattern matches the observed pattern rather well except in central Borneo where overestimation occurs. For the HadCM3Q0/PRECIS simulation, the performance appears relatively better during SON.

Overall, there is greater consistency between the simulated rainfall of HadAM3P/PRECIS and HadCM3Q0/PRECIS, except during DJF season. The negative biases in the HadAM3P/PRECIS during DJF may suggest the model's failure to correctly simulate the winter monsoon winds that bring large amount of rainfall to east coast of Peninsular Malaysia and western Borneo (e.g. Chang et al., 2005; Chen et al., 2013). The HadAM3P/PRECIS also failed to simulate the high intensity of rainfall in the western tip of Borneo during DJF as indicated the APHRODITE data (Fig. 7a). The high intensity of rainfall in this region is caused by the trapped Borneo Vortices over the area especially during January and February (Chen et al., 2013). The underestimation of this maximum rainfall over the region may suggest model's failure to simulate regional circulation features such as the Borneo vortex. In contrast, the HadCM3Q0/PRECIS overestimated rainfall over northeastern Peninsular Malaysia and also central Borneo.

The seasonal spatial correlations between various model simulations (HadAM3P/PRECIS, HadCM3Q0/PRECIS and ERA40/PRECIS) and the APHRODITE dataset for Malaysian rainfall are presented in Fig. 8. The performance of HadAM3P/

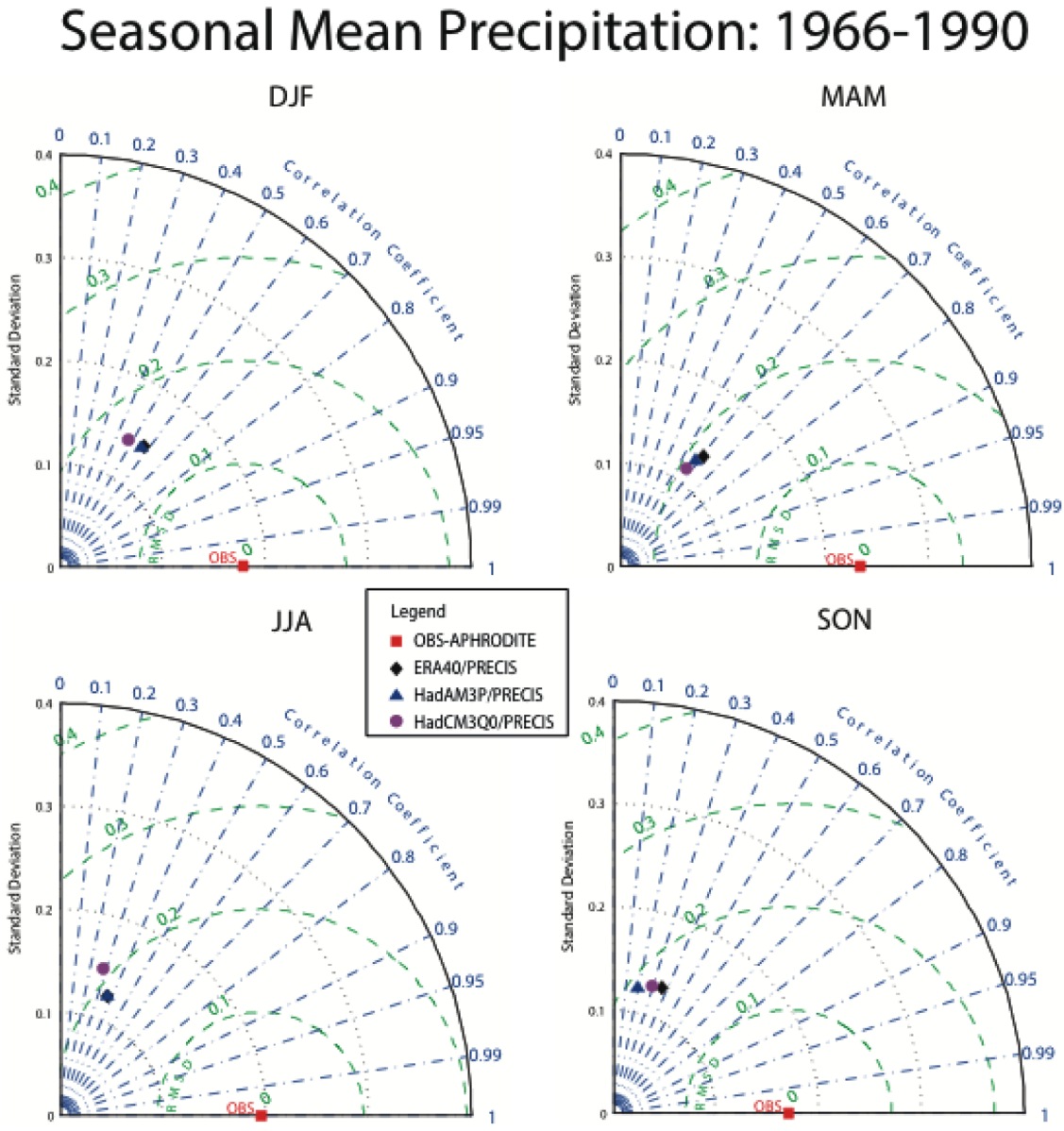

Fig. 8. Taylor diagrams of model simulations (HadAM3P/PRECIS, HadCM3Q0/PRECIS and ERA40/PRECIS) and the APHRODITE dataset for Malaysian seasonal mean rainfall.

PRECIS and HadCM3Q0/PRECIS are comparable and consistent with those ERA40/PRECIS. However, these correlation values are lower than those of temperature shown in Fig. 5. During DJF and MAM seasons, the spatial correlation values range between 0.4-0.5. However, slightly lower correlation values are indicated for JJA and SON (0.3-0.4). These relatively lower values of spatial correlations may reflect the domination of small scales features in the simulated rainfall of both HadAM3P/PRECIS and HadCM3Q0/PRECIS compared to the smoothed APHRODITE rainfall data.

Figure 9 compares monthly climatology of observed APHRODITE rainfall with the HadAM3P/PRECIS and HadCM3Q0/PRECIS simulated rainfall for the 11 sub-regions defined in Fig. 1 for the baseline period (1966-1990). Generally, both HadAM3P/PRECIS and HadCM3Q0/PRECIS simulations capture APHRODITE monthly mean rainfall for each of the sub-region generally well. However, there are some discrepancies that require further discussion. There are large differences between HadAM3P/PRECIS and HadCM3Q0/PRECIS in simulating the APHRODITE monthly rainfall during the winter season in sub-region R1 of the northeast Peninsular Malaysia. In this sub-region, the rainfall peaks in November due to the various rain producing systems (Chen et al., 2013). However, consistent with Fig. 7b, the HadAM3P/PRECIS tends to underestimate the rainfall during the winter monsoon, particularly the maximum rainfall in November. In the HadAM3P/PRECIS simulation, the rain peaks by October, i.e. one month earlier than observed. In contrast, the Had-

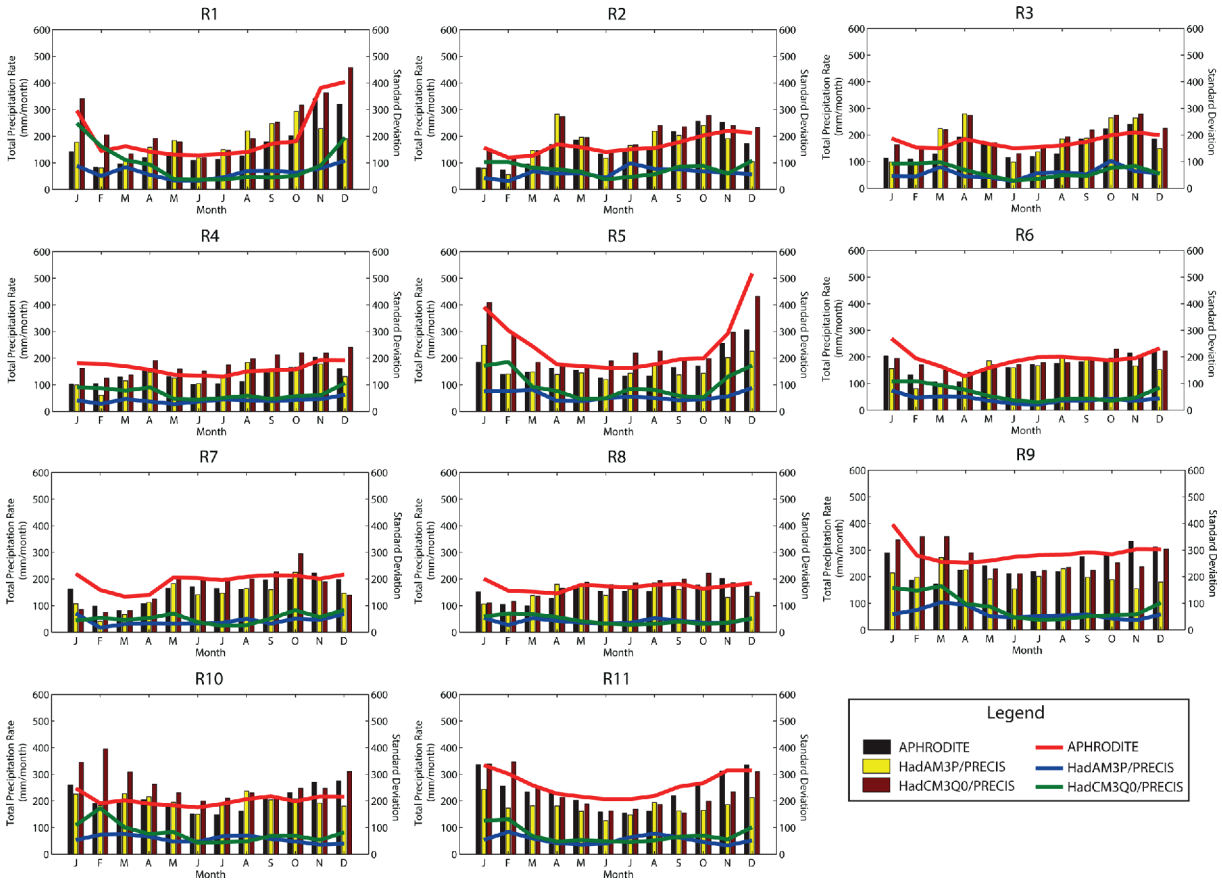

Fig. 9. Comparison between baseline monthly rainfall climatology (left ordinate) of the APHRODITE data and the HadAM3P/PRECIS and HadCM3Q0/PRECIS simulations, averaged over the 11 sub-regions (refer Fig. 1). The observed and simulated interannual variabilities as indicated by the year-to-year standard deviations (right ordinates) are also plotted. Unit is in mm.

CM3Q0/PRECIS overestimated the winter monsoon rainfall, which is consistent with Fig. 7c. The simulated rainfall peaks in December, which is delayed by one month compared with observation. Similar situation is depicted in sub-region R5 of the southeast Peninsular Malaysia. These discrepancies could be related to the model's inability to simulate the monsoon (Chang et al., 2005) and various rain producing systems described in Chen et al. (2013).

In the west coast of Peninsular Malaysia (R2, R3, 4), the HadCM3Q0/PRECIS outperformed HadAM3P/PRECIS. In fact the HadCM3Q0/PRECIS correctly simulated the rainfall maxima in April and in October reasonably well. For areas in the west coast of Peninsular the rainfall does not peak in winter monsoon as in east coast areas because of the blocking effect of the Titiwangsa mountain ranges (e.g. Suhaila and Jemain, 2012). Instead, the rainfall over these areas peaks during the inter-monsoon periods of April and October due to enhanced local convection (Sow et al., 2011). In western Borneo (R10 and R11), the performances of both models appear comparable except during January and February where the HadCM3Q0/PRECIS tends to overestimate the rainfall amount. In northern Borneo (R6, R7 and R8), both models perform reasonably well. Despite, a generally good performance of both models in simulating the monthly mean rainfall, the standard deviations were underestimated in all sub-regions. The annual cycle of these standard deviations are well simulated by the models but not the magnitude.

b. Projections of future climate over Malaysia

(1) Temperature

Figure 10 shows the spatio-temporal variations of projected temperature changes at the end of the 21st century under the SRES A2, A1B and B2 scenarios. Various processes could also influence the spatial variations in rates of warming in the sub-regions. The areas with large temperature changes generally correspond to projected drier region (Fig. 12). However, in the regions with projected increase in precipitation, the rainfall process could trigger various negative feedbacks associated with cloudiness and surface moisture fluxes which then regulates the surface temperature increase over these regions (Hudson and Jones, 2002). Spatial patterns of temperature changes indicate nationwide warming over Malaysia. The annual mean surface air temperature rise by the end of the 21st century ranges from 2.75 to 4.5°C for the A2 and A1B scenario, whereas for the B2 scenario the projected increase is

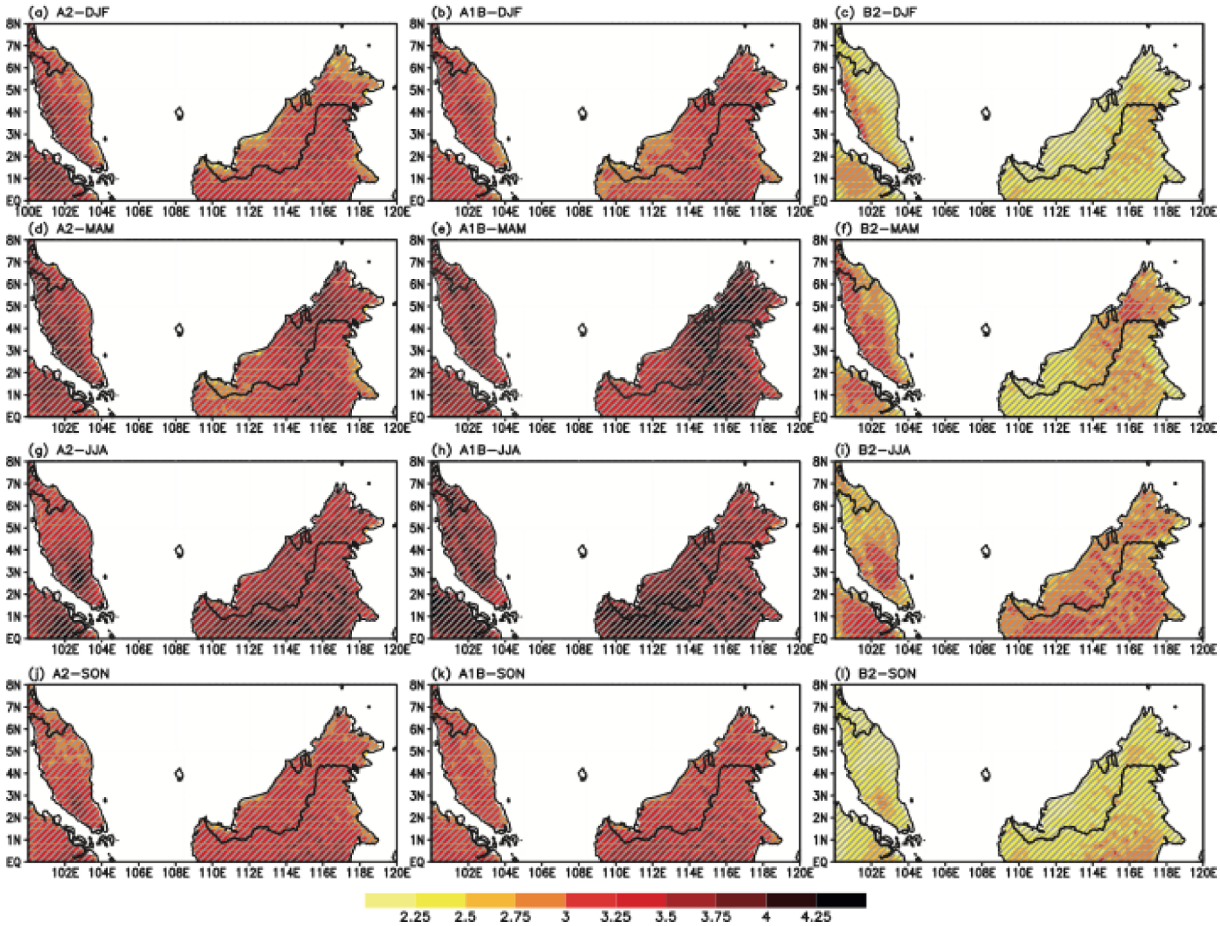

Fig. 10. Spatial patterns of the projected seasonal temperature changes (°C) at the end of the 21st century (2070-2099) simulated by the HadAM3P/PRECIS (A2, B2 scenarios) and HadCM3Q0/PRECIS (A1B scenario). Grey hatching indicates significance at the 95% level.

slightly slower between 2°C and 3.75°C. These projected increases in temperature are considered statistically significant in comparison with the temperatures during the baseline period. In general, the projected increases of temperature are fairly uniform throughout the country. However, there is a tendency for lower increases in coastal regions as compared to interior areas. For example, during DJF, the coastal region along the east coast of Peninsular Malaysia and west coast of Borneo tend to have lower projected temperature by the end of the 21st century compared with the interior regions. There is also seasonal variation where the magnitude of projected warming tends be higher during summer (JJA) and lower during winter season (DJF).

The projected surface air temperatures (mean annual cycles of 11 sub-regions in Malaysia) at the end of the 21st century (2070-2099) for A2, A1B and B2 scenarios are presented in Fig. 11. The figure shows a general increase in temperature over Malaysia with the increment ranges within 1.7 to 4.2°C (Table 1). Temperature increases for all scenarios show similar patterns, but with slightly larger and smaller magnitudes in A1B and B2 scenario, respectively. The simulation produces the highest mean temperature over the southwestern and eastern parts of Peninsular Malaysia (R1, R4 and R5). The western part of Sarawak (R11) has the highest mean temperature amongst the regions of Sabah and Sarawak by the end of 21st century.

(2) Rainfall

The projected changes in rainfall depict considerable spatio-temporal variations by the end of the 21st century (Fig. 12). Generally, the winter rainfall is projected to decrease throughout Malaysia for the A2, A1B and B2 scenarios. However, the rainfall reduction is projected to be higher especially during DJF under the B2 emission scenario despite the fact that B2 is the lowest among the three SRES emission scenarios. Similar condition is depicted for the A2 although the magnitude of reduction is relatively lower. However, for the A1B scenario, the projected rainfall reduction during DJF is largely not significant.

The projected reduction in rainfall for B2 during MAM over Peninsular Malaysia is similar to that of DJF albeit slightly lower magnitude. However, over western Borneo, the projected reduction is not significant except over eastern part of Borneo (Fig. 12f). For A1B scenario, the projected rainfall

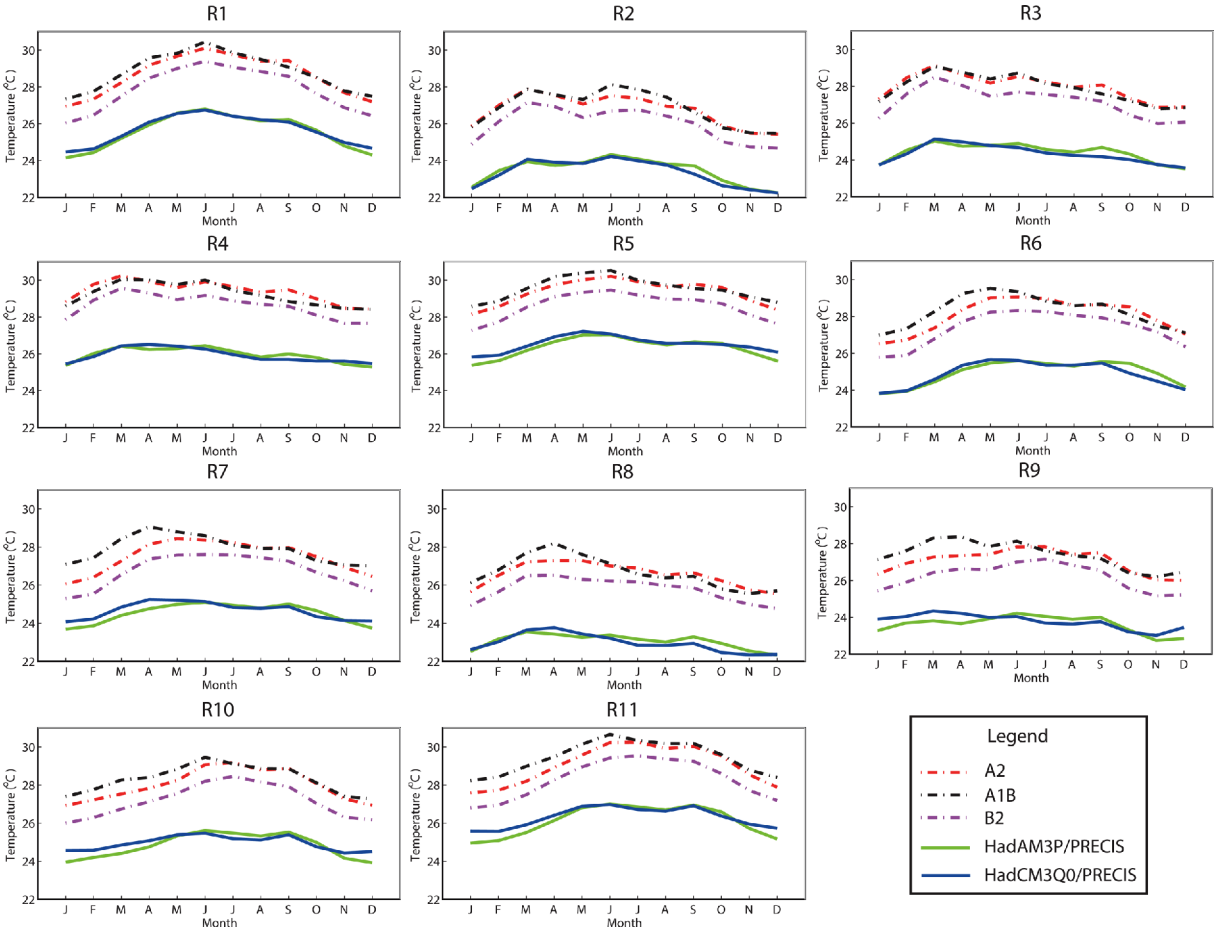

Fig. 11. The comparison of temperature climatology between the HadAM3P/PRECIS and HadCM3Q0/PRECIS baseline (1966-1990) and the future projection of HadAM3P/PRECIS (A2, B2) and HadCM3Q0/PRECIS (B2) by the end of the 21st century (2070-2099) for the 11 sub-regions. Unit is °C.

reduction, depicted over east coast of Peninsular Malaysia and eastern Borneo, is largely not significant. The spatial pattern of projected rainfall reduction in MAM for A2 scenario is similar to that of the A1B scenario except with relatively larger magnitude. Interestingly, in western-central Borneo, rainfall is projected to increase for all three scenarios. For JJA and SON seasons, there is a tendency for projected rainfall to increase particularly for A2 scenario. The projected increase is ~20-40% during JJA and SON over Malaysia, except the eastern coast of Borneo and southern Johor during SON where the rainfall is projected to decrease by ~20-30% for B2 scenario.

Generally, non-uniform rainfall changes among different SRES emission scenarios suggest that, unlike temperature, the responses in hydrological cycle to radiative forcing associated with different SRES emission scenarios are largely not linear. The spatio-temporal pattern of projected rainfall may be due to various processes and feedbacks. Hudson and Jones (2002) suggested that various processes and feedbacks regulate rainfall and surface temperature. However, changes in large-scale phenomena such as the monsoon may also contribute to the projected changes in rainfall. A number of studies have indicated that monsoon is projected to weaken in a warmer climate (e.g. Hung and Kao, 2010; Yao et al., 2010).

The projected changes may be explained in terms of changes in the regional circulation and moisture characteristics. We further investigated this issue by plotting the changes (projection minus baseline simulation) of low-level winds and humidity in Fig. 13. In Fig. 14 we plotted the changes of moisture flux and moisture flux divergence to provide more insights to the changes of projected rainfall depicted in Fig. 12. Climatologically, during DJF the surface circulation over the region is dominated by the northeasterly wind and the monsoon trough is located near to the equator (Chang et al., 2005; Chen et al., 2013). This condition gives rise to generally cyclonic wind flow over the South China Sea. Figure 13 suggests that the projected DJF monsoon wind is generally weaker, indicated by the southwesterly changes at the centre of South China Sea for A2 and A1B and somewhat westerlies changes for the B2 scenario. South of the equator the projected flow changes are easterlies, signifying a weaker cross equatorial flow. This appears consistent with the finding of Tanaka et al. (2005), which reported the weakening of monsoon circulation

Table 1. Projected changes of Malaysian seasonal temperature (°C) and rainfall (%) associated with the three SRES scenarios (A2, A1B and B2) in 11 sub-regions. Bold indicates significance at the 95% level.

Region	Scenarios	Temperature (°C)				Precipitation (%)			
		DJF	MAM	JJA	SON	DJF	MAM	JJA	SON
R1	A2	**2.9**	**3.1**	**3.3**	**3.0**	−14.6	**−22.3**	2.9	**10.7**
	A1B	**2.9**	**3.4**	**3.5**	**2.9**	−14.3	−15.9	−4.2	**10.8**
	B2	**2.0**	**2.4**	**2.6**	**2.1**	**−26.1**	**−28.5**	−5.7	5.4
R2	A2	**3.3**	**3.6**	**3.2**	**3.0**	**−33.6**	−9.5	8.0	6.8
	A1B	**3.4**	**3.6**	**3.8**	**3.2**	−15.5	−6.3	**−22.0**	3.1
	B2	**2.5**	**3.0**	**2.6**	**2.2**	**−41.7**	**−19.2**	−6.4	5.5
R3	A2	**3.6**	**3.8**	**3.6**	**3.2**	**−34.4**	**−11.4**	11.7	3.0
	A1B	**3.5**	**3.8**	**3.8**	**3.2**	−10.8	−7.6	−10.0	**7.9**
	B2	**2.7**	**3.1**	**2.9**	**2.3**	**−45.3**	**−19.5**	−2.7	2.3
R4	A2	**3.5**	**3.6**	**3.5**	**3.2**	**−30.7**	**−15.1**	−10.5	−1.7
	A1B	**3.2**	**3.5**	**3.6**	**3.0**	−19.0	−11.2	−12.3	13.1
	B2	**2.6**	**3.0**	**2.8**	**2.4**	**−36.4**	**−23.1**	**−19.2**	−0.4
R5	A2	**2.8**	**3.0**	**3.2**	**3.0**	**−15.5**	−11.2	**−18.8**	7.3
	A1B	**2.8**	**3.2**	**3.3**	**2.9**	−12.5	−11.4	**−21.4**	7.6
	B2	**2.0**	**2.4**	**2.5**	**2.2**	**−18.6**	**−17.0**	**−28.0**	6.2
R6	A2	**2.8**	**3.2**	**3.4**	**3.0**	**−21.3**	**−37.2**	7.1	**10.0**
	A1B	**3.2**	**3.8**	**3.5**	**3.1**	−15.9	−25.5	7.2	2.0
	B2	**2.0**	**2.6**	**2.8**	**2.3**	**−33.9**	**−35.6**	1.6	−0.4
R7	A2	**2.5**	**3.2**	**3.2**	**2.9**	**−28.3**	**−30.6**	10.0	8.3
	A1B	**3.0**	**3.7**	**3.3**	**3.0**	−10.3	−15.7	−2.6	9.4
	B2	**1.7**	**2.4**	**2.6**	**2.1**	**−31.7**	**−28.5**	−2.5	2.4
R8	A2	**3.2**	**3.9**	**3.6**	**3.3**	**−27.7**	**−13.4**	**13.9**	9.4
	A1B	**3.5**	**4.2**	**3.7**	**3.4**	−4.2	−7.0	3.5	**6.6**
	B2	**2.4**	**3.0**	**2.9**	**2.5**	**−35.9**	**−15.8**	1.3	0.8
R9	A2	**3.2**	**3.5**	**3.6**	**3.3**	**−21.5**	1.9	**13.0**	9.4
	A1B	**3.3**	**4.0**	**3.9**	**3.3**	**−18.1**	−5.2	3.2	11.1
	B2	**2.2**	**2.8**	**2.9**	**2.4**	−30.4	−4.8	1.5	−0.8
R10	A2	**3.0**	**3.0**	**3.5**	**3.2**	**−13.6**	10.5	5.3	7.1
	A1B	**2.9**	**3.4**	**3.9**	**3.3**	**−12.8**	4.1	−1.5	10.4
	B2	**2.1**	**2.3**	**2.8**	**2.2**	**−26.0**	−0.9	−6.0	1.7
R11	A2	**2.7**	**2.7**	**3.3**	**2.9**	**−11.6**	0.7	−5.1	6.3
	A1B	**2.7**	**3.1**	**3.6**	**3.1**	−10.8	−4.1	−14.7	3.7
	B2	**1.9**	**2.1**	**2.6**	**2.1**	**−19.5**	−6.0	−16.4	2.6

at the end of the 21st century due to global warming. However, the projected humidity generally decreases in the domain, due to warmer atmosphere (Fig. 13). This may partially explain the projected reduction in regional rainfall shown in Fig. 12.

Figure 14 shows the projected changes in the vertically integrated moisture flux and the divergence field. It is noted that during DJF, due to the weakened cyclonic monsoon circulation, the South China Sea is dominated by moisture divergence areas. The moisture flux differences are generally pointing southward across the equator, indicating the weakening of the monsoon trough during the DJF and setting the regions drier under warmer climate. The moisture divergence field difference is particular large over northern Borneo for A2 and B2 scenarios which results in much drier climate over this region, as indicated in Fig. 12a, b. The changes in MAM show very similar characteristics to that of the DJF where similar moisture and flow patterns prevail except that the low-level humidity increases slightly over the western

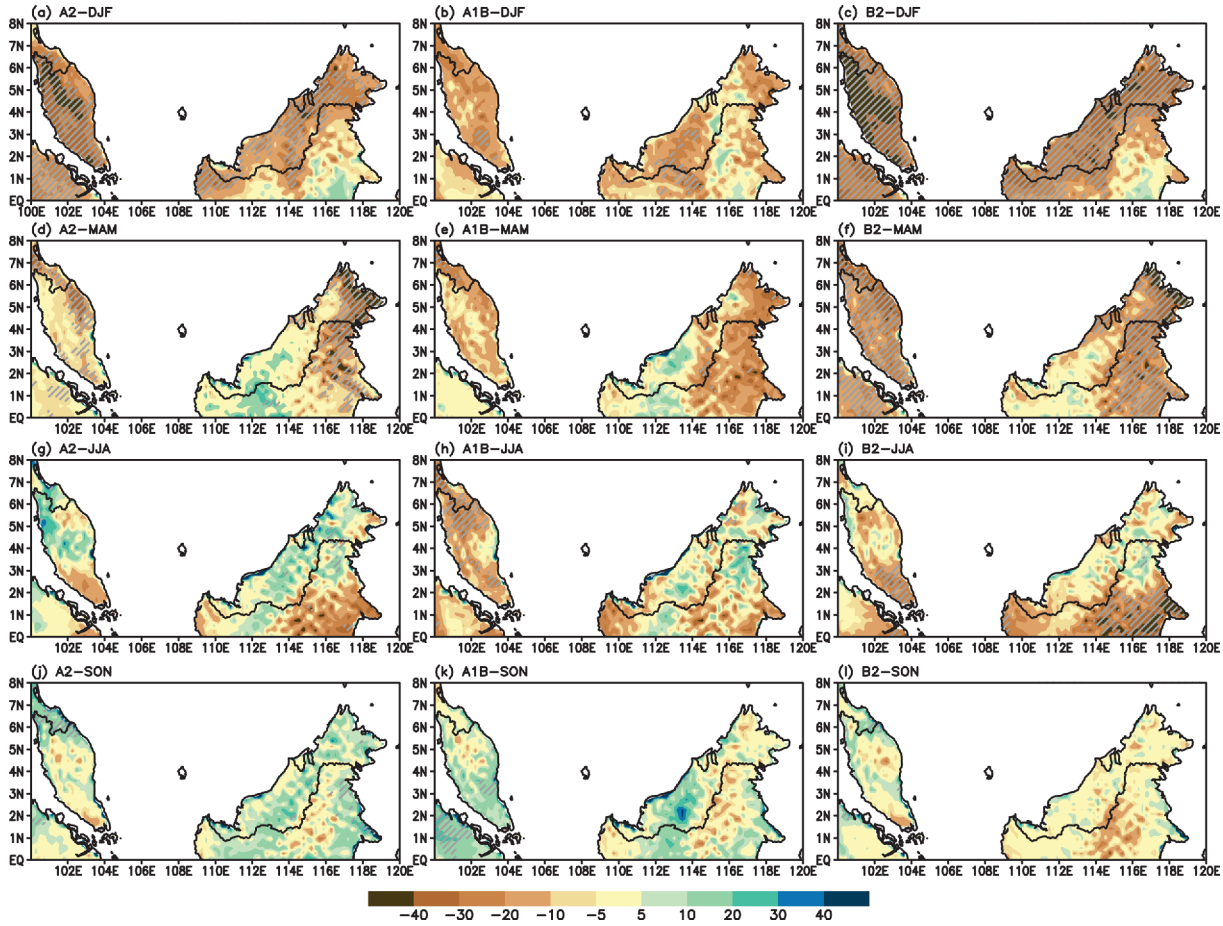

Fig. 12. Spatial patterns of the projected seasonal rainfall changes (%) simulated by the HadAM3P/PRECIS (A2, B2) and HadCM3Q0/PRECIS (A1B). Grey hatching indicates significance at the 95% level.

Borneo, coincides with a marginal increase in rainfall.

During JJA, the climatological low-level circulation south of the equator is predominantly easterly with northward cross-equatorial flow that turns southwesterly to north of the equator. The projected changes of low-level winds show predominantly northwesterly (A2, B2) and westerly (A1B) south of the equator, indicating the weakening of regional summer monsoon flow (Fig. 13). North of the equator, the projected wind changes are southerly over Borneo for both A2 and B2, indicating cyclonic flow changes over the region. These wind changes result in higher relative humidity (Fig. 13) over the western Borneo region that coincides with slightly increased projected rainfall. In addition, generally weakening monsoonal winds during this period could provide favourable conditions for local convection over this region and strengthen rainfall diurnal cycle (e.g. Oki and Musiake, 1994; Sow et al., 2011). However, under the A1B scenario, the southwest monsoonal winds north of the equator are projected to increase and this is likely to be associated with stronger monsoonal wind from the eastern Indian Ocean, which is consistent with the projected decrease in rainfall (Fig. 12) over large part of Peninsular Malaysia. The marginally increase in projected rainfall over the central and northern Borneo and slightly drier condition over the southeast quadrant of the island are likely associated with circulation and moisture changes south of the equator. It is noted that for all scenarios, the relative humidity are projected to increase over the central of Borneo. The moisture flux suggests that the region south of the equator is largely dominated by divergent difference due to weakened local wind (Fig. 14). The moisture flux differences are largely pointing northward and converge towards the central of Borneo. Over the southeast quadrant of the Borneo Island, the moisture field are generally divergent. These patterns of moisture field for all emission scenarios are generally consistent with the projected changes of precipitation over Borneo (Fig. 12). The projected moisture fields of SON generally shows similar pattern with convergence of moisture toward the central of Borneo.

Figure 15 shows the comparison of annual rainfall cycle for the baseline and the projected precipitation over the 11 sub-regions. The projected rainfall of the HadAM3P/PRECIS and HadCM3Q0/PRECIS simulation suggest an overall drier climate over the 11 sub-regions during winter and spring seasons but slightly wetter during summer and autumn. Table 1 provides estimated changes for these sub-regions. In most

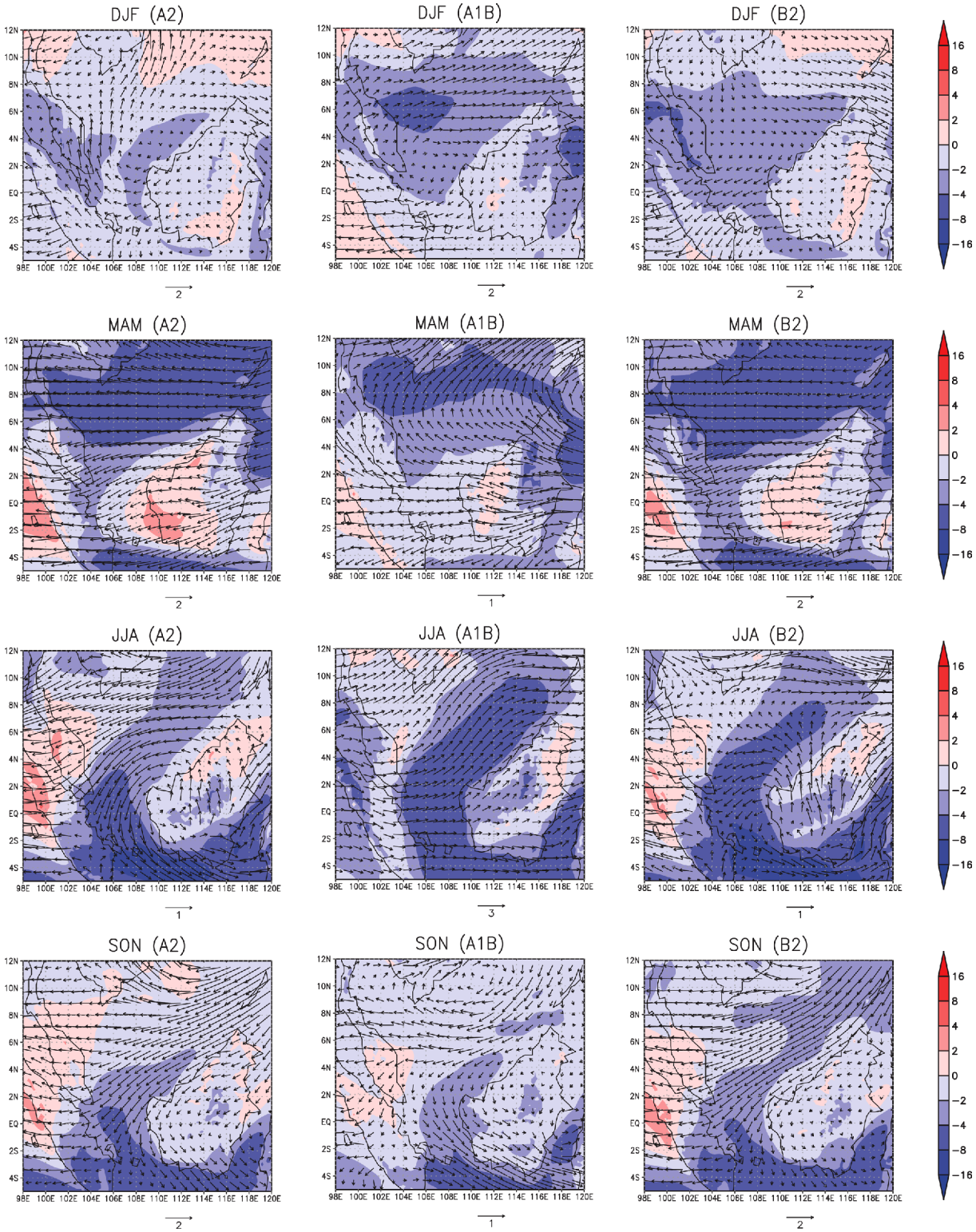

Fig. 13. The projected changes of 850 hPa winds (m s^{-1}) and the relative humidity (%). The projected changes for A2 and B2 scenarios come from the HadAM3P/PRECIS while the A1B come from HadCM3Q0/PRECIS.

sub-regions, the reduction of monthly total rainfall during January and February is about half for the A2 and B2 scenarios. For example, for the R1 sub-region of northeast Peninsular Malaysia in January, the simulated total rainfall is about 200 mm whereas the projected total rainfall for both A2 and B2 is less than 100 mm. In R9 sub-region of western

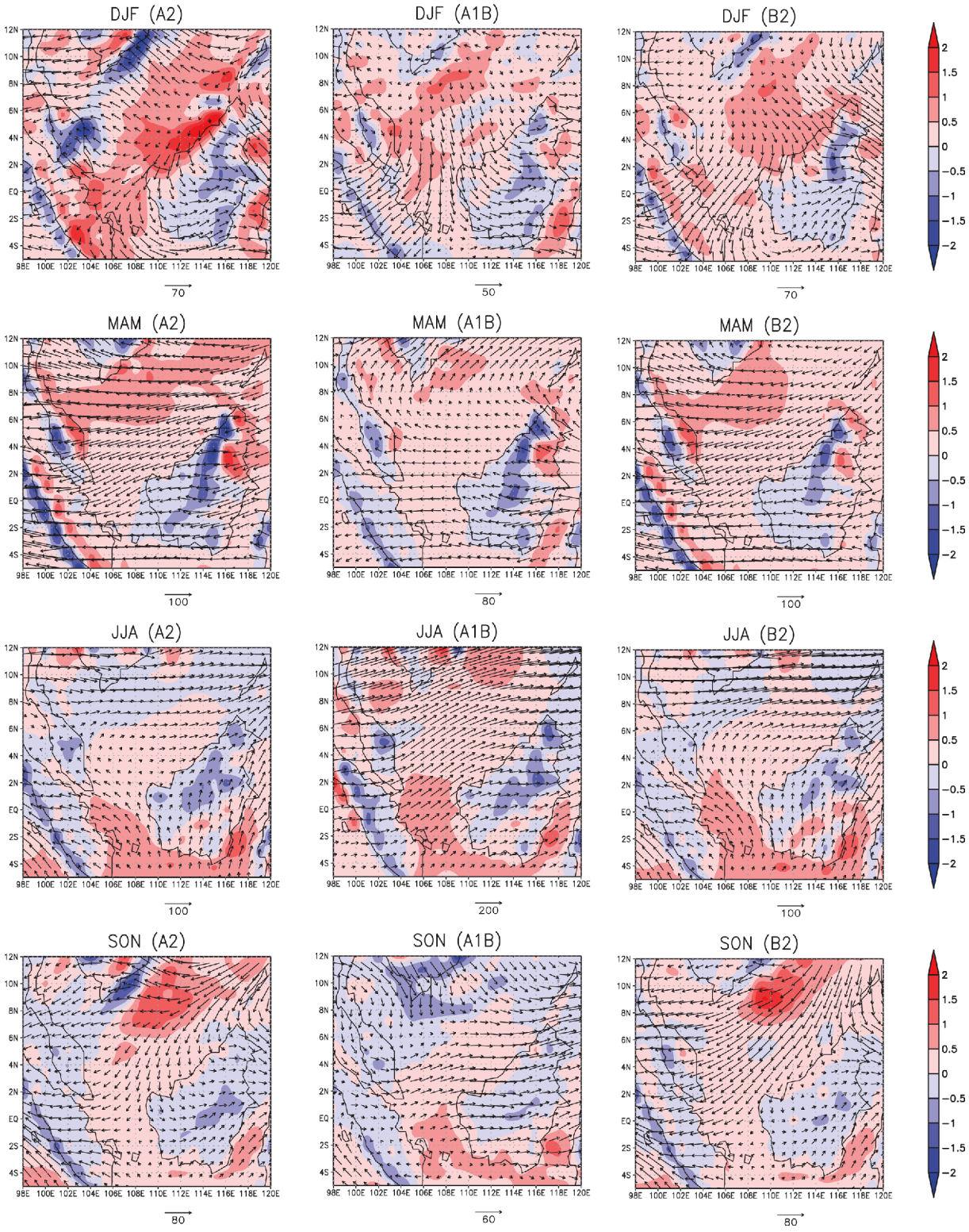

Fig. 14. The projected changes of moisture flux (vector, kg $m^{-1} s^{-1}$) and moisture flux divergence (shaded, 10^{-3} kg $^{-2} s^{-1}$). The projected changes for A2 and B2 scenarios come from the HadAM3P/PRECIS while the A1B come from HadCM3Q0/PRECIS.

Borneo, comparable reduction as that of R1 is projected. Similar situation is depicted for other sub-regions.

4. Conclusions

In this study, we examined the projected temperature and

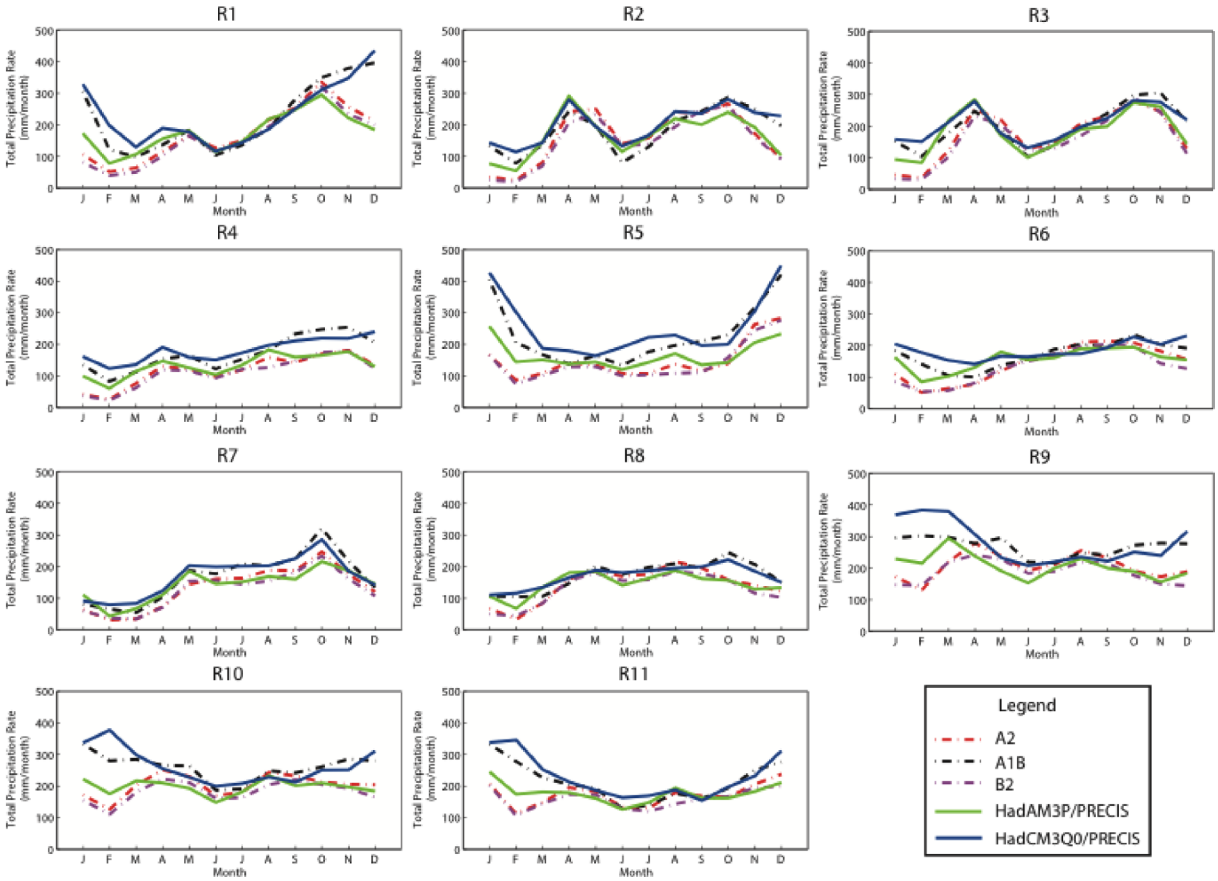

Fig. 15. The comparison of the simulated rainfall climatology of the HadAM3P/PRECIS and HadCM3Q0/PRECIS baseline (1966-1990) and the future projection of A2 and B2 (HadAM3P/PRECIS) and A1B (HadCM3Q0/PRECIS) by the end of the 21st century (2070-2099) for the 11 sub-regions. Unit is in mm.

rainfall changes at the end of 21st century under the SRES A2, A1B and B2 emission scenarios using the HadAM3P/PRECIS and HadCM3Q0/PRECIS. Generally, the downscaled climate patterns during the baseline period compared reasonably well to those of the APHRODITE data. The performances of HadAM3P/PRECIS and HadCM3Q0/PRECIS in simulating mean surface temperature are consistent to those of ERA40/PRECIS. However, there were overall cold biases in the temperature simulation because of the systematic error in PRECIS. However, compared with temperature, the skill in simulating precipitation is lower. Noticeably, the models produced mesoscale features and this partially contributed to the lower correlation when compared to the smoothed APHRODITE data. Generally, the HadCM3Q0/PRECIS produces slightly wetter condition compared with the APHRODITE especially over central Borneo and northeastern Peninsular Malaysia. In contrast, the HadAM3P/PRECIS produces slightly drier condition especially over western Borneo during DJF and SON seasons. The discrepancies between the simulated rainfalls and APHRODITE data may be attributed to model's failure to correctly represent various feedback processes (e.g. Hudson and Jones, 2002). In addition, the models may not simulate the regional circulation system (e.g. Chang et al., 2005) and the rain producing systems (e.g. Chen et al., 2013) especially during winter monsoon.

The projected changes in temperature indicate spatio-temporal variation but overall warming throughout Malaysia by the end of the 21st century, which is incremental according to the greenhouse forcing. The projected temperature increment varies from 2.5 to 3.9°C, 2.7 to 4.2°C and 1.7 to 3.1°C for the SRES A2, A1B and B2 scenarios, respectively. In contrast, the precipitation response to greenhouse forcing appears non-incremental. The projected changes in rainfall by the end of the 21st century indicate spatio-temporal variability as well as dependence on the emission scenarios. Overall, drier condition is projected throughout Malaysia during DJF and MAM and generally wetter condition in JJA and SON. These projected changes in rainfall can be related to the weakening of the monsoon circulations, which in turn alters the pattern of regional moisture convergences in the region. During DJF ~20-40% decrease of rainfall is projected over Peninsular Malaysia and Borneo, particularly for the A2 and B2 emission scenarios. The reduction in rainfall is larger for the B2 scenario compared to A2 scenario. During JJA and SON the projected rainfall increase is ~20-40% across most regions in Malaysia, especially for A2 and A1B scenarios. Despite the usefulness of

these results, one needs to take into consideration the issue of uncertainties in the projections. It is well known that regional climate scenarios have many uncertainties of various sources including inter-model differences e.g. CMIP3 and CMIP5 models (Knutti and Sedlacek, 2013) and natural and anthropogenic aerosol forcing (Lau, 2015). There is an obvious limitation of this study with respect to uncertainties from inter-model comparison as it employed only two GCMs i.e. HadAM3P and HadCM3Q0. In future study, the uncertainty from aerosol forcing should be investigated because at the regional scale the impact of aerosol forcing on monsoon circulation is strong (Lau, 2014; Kim et al., 2016).

Acknowledgements. This research was funded by Universiti Kebangsaan Malaysia ICONIC-2013-001, AP-2013-005 grants and the BK21 plus Project of the Graduate School of Earth Environmental Hazard System, Pukyong National University, Busan, Korea. The provision of the PRECIS regional model and associated support by the Met Office UK are noted with thanks. We thank two anonymous reviewers for their constructive suggestions.

Edited by: Song-You Hong, Kim and Yeh

References

Aldrian, E., and R. D. Susanto, 2003: Identification of three dominant rainfall regions within Indonesia and their relationship to sea surface temperature. *Int. J. Climatol.*, **23**, 1435-1452.

Alves, L. M., and J. Marengo, 2010: Assessment of regional seasonal predictability using the PRECIS regional climate modeling system over South America. *Theor. Appl. Climatol.*, **100**, 337-350.

Ashok, K., Z. Guan, and T. Yamagata, 2001: Impact of the Indian Ocean Dipole on the relationship between Indian Ocean monsoon rainfall and ENSO. *Geophys. Res. Lett.*, **28**, 4499-4502.

Behera, S. K., J.-J. Luo, and T. Yamagata, 2008: The Unusual IOD Event of 2007. *Geophys. Res. Lett.*, **35**, L14S11, doi:10.1029/2008GL034122.

Chang, C. P., Z. Wang, J. Ju, and T. Li, 2003: On the relationship between western Maritime Continent rainfall and ENSO during northern winter. *J. Climate*, **17**, 665-672.

_____, P. A. Harr, and H. J. Chen, 2005: Synoptic disturbances over the equatorial South China Sea and western maritime continent during boreal winter. *Mon. Wea. Revi*, **133**, 489-503.

Chen, T. C., J.-D. Tsay, M.-C. Yen, and J. Matsumoto, 2013: The winter rainfall of Malaysia. *J. Climate*, **26**, 936-958.

Collins, M., S. F. B. Tett, and C. Cooper, 2001: The internal climate variability of HadCM3, a version of the Hadley Centre coupled model without flux adjustments. *Clim. Dynam.*, **17**, 61-81.

Dickinson, R. E., R. M. Errico, F. Giorgi, G. T. Bates, 1989: A regional climate model for the western United States. *Climatic Change*, **15**, 383-422.

Giorgi, F., and B. Hewitson, 2001: Regional climate information-evaluation and projections. *Climate Change 2001: The Scientific Basis. Contribution of Working Group to the Third Assessment Report of the Intergouvernmental Panel on Climate Change,* J. Houghton et al. Eds., Cambridge University Press, 585-638.

_____, C. Jones, and G. R. Asrar, 2009: Addressing climate information needs at the regional level: the CORDEX framework. *WMO Bull.*, **58**, 177-183.

Gong, D. Y, and C. H. Ho, 2002: The Siberian High and climate change over middle to high latitude Asia. *Theor. Appl. Climatol.*, **72**, 1-9.

Gordon, C., C. Cooper, C. A. Senior, H. Banks, J. M. Gregory, T. C. Johns, J. F. B. Mitchell, and R. A. Wood, 2000: The simulation of SST, sea ice extents and ocean heat transports in a version of the Hadley Centre coupled model without flux adjustments. *Clim. Dynam.*, **16**, 147-168.

Hendon, H. H., 2003: Indonesian rainfall variability: Impacts of ENSO and local air-sea interaction. *J. Climate*, **16**, 1775-1790.

Hu, Z.-Z., L. Bengtsson, and K. Arpe, 2000a: Impact of global warming on the Asian winter monsoon in a coupled GCM. *J. Geophys. Res.*, **105**, 4607-4624.

_____, M. Latif, E. Roeckner, and L. Bengtsson, 2000b: Intensified Asian summer monsoon and its variability in a coupled model forced by increasing greenhouse gas concentrations. *Geophys. Res. Lett.*, **27**, 2681-2684.

Hudson, D. A., and R. G. Jones, 2002: *Regional climate model simulation of present-day and future climates of southern Africa.* Hadley Centre Technical Note 39, 41 pp.

Hung, C. W., and P. K. Kao, 2010: Weakening of the Winter Monsoon and Abrupt Increase of Winter Rainfalls over Northern Taiwan and Southern China in the Early 1980s. *J. Climate*, **23**, 2357-2367.

IPCC, 2007: Summary for Policymakers. *Climate Change 2007: The Physical Science Basis. Contribution of Working Group I to the Fourth Assessment Report of the Intergovernmental Panel on Climate Change,* S. Solomon, et al. Eds., Cambridge University Press, 18 pp.

_____, 2013: *Climate Change 2013: The Physical Science Basis. Contribution of Working Group I to the Fifth Assessment Report of the Intergovernmental Panel on Climate Change*, T. F. Stocker et al. Eds., Cambridge University Press, Cambridge, 1535 pp.

Johns, T. C., R. E. Carnell, J. F. Crossley, J. M. Gregory, J. F. B. Mitchell, C. A. Senior, S. F. B. Tett, and R. A. Wood, 1997: The second Hadley Centre coupled ocean-atmosphere GCM: model description, spinup and validation. *Clim. Dynam.*, **13**, 103-134.

_____, and Coauthors, 2003: Anthropogenic climate change for 1860 to 2100 simulated with the HadCM3 model under updated emissions scenarios. *Clim. Dynam.*, **20**, 583-612.

Jones, R. G., M. Noguer, D. C. Hassell, D. Hudson, S. S. Wilson, G. J. Jenkins, and J. F. B. Mitchell, 2004: *Generating high resolution climate change scenarios using PRECIS*. Met Office Hadley Centre, 35 pp.

Juneng, L., and F. T. Tangang, 2005: Simulation of near-equatorial Typhoon Vamei. *J. Eng. Sci.*, **1**, 97-109.

_____, and _____, 2010: Long-term trends of winter monsoon synoptic circulations over the maritime continent: 1962-2007. *Atmos. Sci. Lett.*, **11**, 199-203.

Kim, M. K., W. K. M. Lau, K. M. Kim, J. Sang, Y. H. Kim, and W. S. Lee, 2016: Amplification of ENSO effects on Indian summer monsoon by absorbing aerosols. *Clim. Dynam.*, **45**, 2657-2671.

Knutti, R., and J. Sedlacek, 2013: Robustness and uncertainties in the new CMIP5 climate model projections. *Nat. Clim. Change*, **3**, 369-373.

Kwan, M. S., F. T. Tangang, and L. Juneng, 2014: Present-day regional climate simulation over Malaysia and western Maritime Continent region using PRECIS forced with ERA40 reanalysis. *Theor. Appl. Climatol.*, **115**, 1-14.

Lau, W, 2014: Atmospheric science: Desert dust and monsoon rain. *Nature Geoscience*, **7**, 255-256.

_____, 2015: The aerosol-monsoon climate system of Asia: A new paradigm. *J. Meteor. Res.*, **30**, 1-11.

Massey, M., R. Jones, F. E. L. Otto, T. Aina, S. Wilson, J. M. Murphy, D. Hassell, Y. H. Yamazaki, and M. R. Allen, 2015: Weather@home—development and validation of a very large ensemble modelling system for probabilistic event attribution. *Quart. J. Roy. Meteor. Soc.,* **141**, 1528-1545.

McBride, J. L., M. R. Haylock, and N. Nicholls, 2003: Relationships

between the Maritime Continent heat source and the El Niño-Southern Oscillation phenomenon. *J. Climate*, **16**, 2905-2914.

Meehl, G. A., and J. M. Arblaster, 2003: Mechanisms for projected future changes in south Asian monsoon precipitation. *Clim. Dynam.*, **21**, 659-675.

_____, and _____, 2011: Decadal variability of Asian-Australian monsoon-ENSO-TBO relationships. *J. Climate*, **24**, 4925-4940.

_____, and Coauthors, 2007: Global Climate Projections. *Climate Change 2007-The Physical Science Basis. Contribution of Working Group I to the Fourth Assessment Report of the Intergovernmental Panel on Climate Change,* S. Solomon et al. Eds., Cambridge University Press, 749-846.

Moron, V., A. W. Robertson, and R. Boer, 2009: Spatial Coherence and Seasonal Predictability of Monsoon Onset over Indonesia. *J. Climate*, **22**, 840-850.

Nakićæenović, N., and Coauthors, 2000: *IPCC Special Report on Emissions Scenarios: A Special Report of Working Group III of the Intergovernmental Panel on Climate Change*. Cambridge University Press, 599 pp.

Oki, T., and K. Musiake, 1994: Seasonal change of the diurnal cycle of precipitation over Japan and Malaysia. *J. Appl. Meteor. Climatol.,* **33**, 1445-1463.

Pope, V. D., M. L. Gallani, P. R. Rowntree, and R. A. Stratton, 2000: The impact of new physical parameterizations in the Hadley Centre climate model — HadAM3. *Clim. Dynam.*, **16**, 123-146.

Randall, D. A., and Coauthors, 2007: Cilmate Models and Their Evaluation. *Climate Change 2007: The Physical Science Basis. Contribution of Working Group I to the Fourth Assessment Report of the Intergovernmental Panel on Climate Change,* S. Solomon et al. Eds.,Cambridge University Press, 591-663.

Ravindranath, N. H., and J. A. Sathaye, 2002: Climate Change and Developing Countries. *Advances in Global Change Research,* M. Beniston et al. Eds., Kluwer Academic Publishers, 247-265.

Robertson, A., V. Moron, J. Qian, C. P. Chang, F. Tangang, E. Aldrian, T. Y. Koh, and L. Juneng, 2011: The Maritime Continent Monsoon. *The Global Monsoon System: Research and Forecast,* C. Chang et al. Eds., World Scientific, 85-98.

Rupa Kumar, K., A. K. Sahai, K. Krishna Kumar, S. K. Patwardhan, P. K. Mishra, J. V. Revadekar, K. Kamala, and G. B. Pant, 2006: High-resolution climate change scenarios for India for the 21st century. *Current Sci.*, **90**, 334-345.

Salimun, E., F. Tangang, L. Juneng, S. K. Behera, and W. Yu, 2014: Differential impacts of conventional El Niño *versus* El Niño Modoki on Malaysian rainfall anomaly during winter monsoon. *Int. J. Climatol.*, **34**, 2763-2774.

_____, _____, _____, F. W. Zwiersb, and W. J. Merryfield, 2015: Skill evaluation of the CanCM4 and its MOS for seasonal rainfall forecast in Malaysia during the early and late winter monsoon periods. *Int. J. Climatol.*, doi: 10.1002/joc.4361.

Suhaila, J., and A. A. Jemain, 2012: Spatial Analysis of Daily Rainfall Intensity and Concentration Index in Peninsular Malaysia. *Theor. Appl. Climatol.*, **108**, 235-245.

Sow, K. S., L. Juneng, and F. Tangang, 2011: Numerical simulation of a severe late afternoon thunderstorm over Peninsular Malaysia. *Atmos. Res.*, **99**, 248-262.

Stratton, R. A., 1999: A high resolution AMIP integration using the Hadley Centre model HadAM2b. *Clim. Dynam.*, **15**, 9-28.

Takle, E. S., and Coauthors, 1999: Project to Intercompare Regional Climate Simulations (PIRCS): Description and initial results. *J. Geophys. Res.*, **104**, 19443-19461.

Tan, M. L., A. L. Ibrahim, Z. Duan, A. P. Cracknell, and V. Chaplot, 2015: Evaluation of Six High-Resolution Satellite and Ground-Based Precipitation Products over Malaysia. *Remote Sens.*, **7**, 1504-1528.

Tanaka, H. L., N. Ishizaki, and D. Nohara, 2005: Intercomparison of the intensities and trends of Hadley, Walker and monsoon circulations in the global warming projections. *SOLA*, **1**, 77-80.

Tangang, F. T., and L. Juneng, 2004: Mechanisms of Malaysian rainfall anomalies. *J. Climate*, **17**, 3616-3622.

_____, _____, and S. Ahmad, 2007: Trend and interannual variability of temperature in Malaysia: 1961-2002. *Theor. Appl. Climatol.*, **89**, 127-141.

_____, _____, S. Salimun, M. S. Kwan, J. L. Loh, H. Muhamad, 2012: Climate Change and Variability over Malaysia: Gaps in Science and Research Information. *Sains Malaysiana*, **41**, 1355-1366.

Trenberth, K. E., and Coauthors, 2007: Observations: Surface and Atmospheric Climate Change. *Climate Change 2007-The Physical Science Basis. Contribution of Working Group I to the Fourth Assessment Report of the Intergovernmental Panel on Climate Change,* S. Solomon et al. Eds., Cambridge University Press, 237-336.

Waliser, D. E., and Coauthors, 2003: AGCM simulations of intraseasonal variability associated with the Asian summer monsoon. *Clim. Dynam.*, **21**, 423-446.

Wang, B., R. Wu, and T. Li, 2003: Atmosphere-warm ocean interaction and its impacts on Asian-Australian monsoon variation. *J. Climate*, **16**, 1195-1211.

Wu, M. C., K. H. Yeung, and Y. K. Leung, 2007: Changes in the East Asian winter atmospheric circulation. *Presented in International Conference on Climate Change*, Hong Kong, 29-31.

Xu, M., C. P. Chang, C. Fu, Y. Qi, A. Robock, D. Robinson, and H. Zhang, 2006: Steady decline of East Asian monsoon winds, 1969-2000: evidence from direct ground measurements of wind speed. *J. Geophys. Res.*, **111**, D24111, doi: 10.1029/2006D007337.

Yatagai, A., K. Kamiguchi, O. Arakawa, A. Hamada, N. Yasutomi, and A. Kitoh, 2012: APHRODITE: Constructing a Long-term Daily Gridded Precipitation Dataset for Asia Based on a Dense Network of Rain Gauges. *Bull. Amer. Meteor. Soc.*, **93**, 1401-1415.

Yao, C., W. Qian, S. Yang, and Z. Lin, 2010: Regional features of precipitation over Asia and summer extreme precipitation over Southeast Asia and their associations with atmospheric-oceanic conditions. *Meteor. Atmos. Phys.*, **106**, 57-73.

Yu, R., and T. Zhou, 2007: Seasonality and three-dimensional structure of the interdecadal change in East Asian monsoon. *J. Climate*, **20**, 5344-5355.